Time-Resolved Ultraviolet Resonance Raman Study of the Photolysis of Carbomonoxyhemoglobin. Relaxation of the Globin Structure

S. Kaminaka, T. Ogura, and T. Kitagawa*

Contribution from the Institute for Molecular Science, Okazaki National Research Institutes, Myodaiji, Okazaki, 444 Japan. *Received December 13, 1988*

Abstract: Dynamical features of quaternary structure changes of carbomonoxyhemoglobin (COHb) after photolysis were followed by observing resonance-enhanced Raman bands of the aromatic residues in ultraviolet excitation. The Raman scattering was excited by 10-ns pulses at 218 nm, which were obtained from the second H_2 Raman shift of the fourth harmonic of a Nd:YAG laser, while CO was photodissociated by 10-ns pulses at 419 nm generated by a nitrogen-laser-pumped dye laser or by pulses at 436 nm generated from the first H_2 Raman shift of the second harmonic of the Nd:YAG laser. The delay time (Δt_d) from the photolysis pulse to the Raman probe pulse was varied from −100 to 500 μs. The observed spectra obtained for $\Delta t_d = -100$ μs and 10 ns were the same as each other and as that obtained without the pump beam, contrary to expectations based on the reported 7-ns change of the protein structure, but the spectral pattern did change when Δt_d changed from 10 to 20 μs; the bands at 1613 and 1011 cm^{-1} decreased in intensity, and the band at 878 cm^{-1} shifted to 883 cm^{-1}. These spectral changes appeared as a smooth monotonous function of time, suggesting the absence of an intermediate around $\Delta t_d = 10$ μs. A similar spectral change was also observed upon addition of an effector (inositol hexaphosphate) to metHbF. Accordingly, the observed changes of the UV resonance Raman spectra were attributed to a quaternary structure change, presumably to a status change of β37-Trp and α42-Tyr at the α_1–β_2 subunit interface.

The structural mechanism of hemoglobin cooperativity continues to be a subject of extensive studies,[1-9] since it serves as a typical model of general allostery.[10] The rich information on hemoglobin (Hb) has offered a fertile ground for scrutinizing our ideas about how the binding or dissociation of a ligand in a particular heme iron is communicated to other hemes and how this changes their oxygen affinity. A number of experimental data have been satisfactorily explained by assuming a reversible transition between the low-affinity (T) and high-affinity quaternary structures (R).[11] Since carbomonoxyhemoglobin (COHb) and deoxyHb adopt the R and T states, respectively,[1b] the photolysis of the heme CO adduct provides a means for studying the dynamical features of the quaternary structure transition.[12-14] Structural evolution following the photolysis of COHb has been monitored mainly by optical absorption[14-18] and visible resonance Raman (RR) techniques.[19-21]

Previously, it was demonstrated[22,23] that the Fe–histidine (F8) stretching (ν_{Fe-His}) band serves as a marker for the quaternary structure of deoxyHb. It is known that this mode[5] as well as other porphyrin modes[19-22] exhibits time-dependent frequency shifts after the photolysis of COHb. Furthermore, the relation between the ν_{Fe-His} frequency and the oxygen affinity was interpreted in terms of the strain imposed on the Fe–histidine (F8) (Fe–His) bond by the globin.[9a,b] On the other hand, the quaternary structure of Hb is defined by the relative arrangements of four subunits and the hydrogen bonds and salt bridges between the subunits.[1,24] The ^1H NMR signal of α42-Tyr, which forms a hydrogen bond with β99-Asp at the α_1–β_2 interface in the T structure but is free in the R structure, has served as a diagnostic marker for the quaternary structure.[25] The question is whether the change in the Fe–His bond really triggers a change at the α_1–β_2 interface or not. In order to answer this, it is essential to monitor dynamical features of the globin and heme structures with the same technique. Unfortunately, NMR spectroscopy cannot follow structural changes as fast as one microsecond, but Raman spectroscopy can.

Ultraviolet (UV) excitation of Raman scattering has recently been shown to probe resonance-enhanced Raman bands of protein aromatic side chains.[26-29] Strong enhancement is reported for tryptophan (Trp), tyrosine (Tyr), and phenylalanine (Phe) residues upon excitation around 220–200 nm.[26a] Spiro and co-workers[8a,b] applied the UV RR technique to study evolution of the protein structure after photolysis of COHb and concluded that the R to T change at the α_1–β_2 interface was apparently completed within 7 ns after the photolysis. This observation is not compatible with

* Author to whom correspondences should be addressed.

(1) (a) Perutz, M. F. *Nature (London)* **1970**, *228*, 726–734. (b) Perutz, M. F. *Annu. Rev. Biochem.* **1979**, *48*, 327–386.
(2) Frauenfelder, H.; Wolyness, P. G. *Science* **1985**, *229*, 337–345.
(3) Agmon, N.; Hopfield, J. J. *J. Chem. Phys.* **1983**, *79*, 2042–2053.
(4) Johnson, M. L.; Turner, B. W.; Ackers, G. K. *Proc. Natl. Acad. Sci. U.S.A.* **1984**, *81*, 1093–1097.
(5) (a) Friedman, J. M. *Science* **1985**, *228*, 1273–1280. (b) Friedman, J. M.; Rousseau, D. L. In *Biological Applications of Raman Spectroscopy*; Spiro, T. G., Ed.; Wiley: New York, 1988; pp 133–215.
(6) (a) Viggiano, G.; Ho, C. *Proc. Natl. Acad. Sci. U.S.A.* **1979**, *76*, 3673–3677. (b) Miura, S.; Ho, C. *Biochemistry* **1982**, *21*, 6280–6287.
(7) Inubushi, T.; D'Ambrosio, C.; Ikeda-Saito, M.; Yonetani, T. *J. Am. Chem. Soc.* **1986**, *108*, 3799–3803.
(8) (a) Copeland, R. A.; Dasgupta, S.; Spiro, T. G. *J. Am. Chem. Soc.* **1985**, *107*, 3370–3371. (b) Dasgupta, S.; Copeland, R. A.; Spiro, T. G. *J. Biol. Chem.* **1986**, *261*, 10960–10962.
(9) (a) Matsukawa, S.; Mawatari, K.; Yoneyama, Y.; Kitagawa, T. *J. Am. Chem. Soc.* **1985**, *107*, 1108–1113. (b) Kitagawa, T. *Pure Appl. Chem.* **1987**, *59*, 1285–1294. (c) Kaminaka, S.; Ogura, T.; Kitagishi, K.; Yonetani, T.; Kitagawa, T. *J. Am. Chem. Soc.* **1989**, *111*, 3787–3794.
(10) Monod, J.; Wyman, J.; Changeux, J. P. *J. Mol. Biol.* **1985**, *12*, 88–118.
(11) Shulman, R. G.; Hopfield, J. J.; Ogura, S. *Q. Rev. Biophys.* **1975**, *8*, 325–420.
(12) Sawicki, C. A.; Gibson, Q. H. *J. Biol. Chem.* **1976**, *251*, 1533–1542.
(13) Cho, K. C.; Hopfield, J. J. *Biochemistry* **1979**, *18*, 5826–5833.
(14) Hofrichter, J.; Sommer, J. H.; Henry, E. R.; Eaton, W. A. *Proc. Natl. Acad. Sci. U.S.A.* **1983**, *80*, 2235–2239.
(15) (a) Martin, J. L.; Mingus, A.; Poyart, C.; Lecarpentier, Y.; Astier, R.; Antonetti, A. *Proc. Natl. Acad. Sci. U.S.A.* **1983**, *80*, 173–177. (b) Petrich, J. W.; Martin, J. L.; Houde, D.; Poyart, C.; Orszag, A. *Biochemistry* **1987**, *26*, 7914–7923.
(16) Greene, B. I.; Hochstrasser, R. M.; Weisman, R. B.; Eaton, W. A. *Proc. Natl. Acad. Sci. U.S.A.* **1978**, *75*, 5255–5259.
(17) Shank, C. V.; Ippen, E. P.; Bersohn, R. *Science* **1976**, *193*, 50–51.
(18) Reynolds, A. H.; Rentzepis, P. M. *Biophys. J.* **1982**, *38*, 15–18.
(19) (a) Dallinger, R. F.; Nestor, J. R.; Spiro, T. G. *J. Am. Chem. Soc.* **1978**, *100*, 6251–6252. (b) Terner, J.; Stong, J. D.; Spiro, T. G.; Nagumo, M.; Nicol, M. F.; El-Sayed, M. A. *Proc. Natl. Acad. Sci. U.S.A.* **1981**, *78*, 1313–1317. (c) Stein, P.; Terner, J.; Spiro, T. G. *J. Phys. Chem.* **1982**, *86*, 168–170. (d) Dasgupta, S.; Spiro, T. G. *Biochemistry* **1986**, *25*, 5941–5948.
(20) (a) Lyons, K. B.; Friedman, J. M.; Fleury, P. A. *Nature (London)* **1978**, *275*, 565–566. (b) Friedman, J. M.; Rousseau, D. L.; Ondrias, M. R. *Annu. Rev. Phys. Chem.* **1982**, *33*, 471–491. (c) Friedman, J. M.; Scott, T. W.; Stepnoski, R. A.; Ikeda-Saito, M.; Yonetani, T. *J. Biol. Chem.* **1983**, *258*, 10564–10572. (d) Scott, T. W.; Friedman, J. M. *J. Am. Chem. Soc.* **1984**, *106*, 5677–5687. (e) Ondrias, M. R.; Friedman, J.; Rousseau, D. L. *Science* **1983**, *220*, 615–617.
(21) Woodruff, W. H.; Farquharson, S. *Science* **1978**, *201*, 831–833.
(22) Irwin, M. J.; Atkinson, G. H. *Nature (London)* **1981**, *293*, 317–318.

0002-7863/90/1512-23$02.50/0

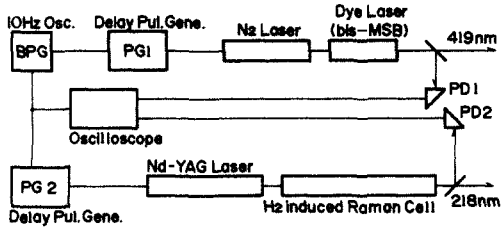

Figure 1. Layout of the time-resolved UV RR measurement system: BPG, 10-Hz pulse generator (1-MHz quartz oscillator); PG1, pulse generator for firing the N_2 laser; PG2, pulse generator for firing Nd:YAG laser; PD1, photodiode for detecting the 419-nm pulse; PD2, photodiode for detecting the 218-nm pulse.

the common view that the ligand binding at the heme iron is communicated to the subunit interface through the Fe–His bond, and if its were true, presently accepted ideas about the structural mechanism of the Hb cooperativity would have to be fundamentally revised. Accordingly, we decided to reexamine the observation of Spiro and co-workers.[8a,b] We report here that such a change of the protein structure at the subunit interface takes place in the interval between 10 and 20 μs after the photolysis. While this paper was under review, Su et al.[30] published a paper that retracted the previous paper[8a,b] from their group. The present results are partly consistent with their new conclusion in a sense that the protein structural change occurs ca. 10 μs after photolysis but do not support their claim that an intermediate is formed around 10 μs after photolysis.

Experimental Section

The layout of the present observation system is illustrated in Figure 1. The excitation light for the Raman scattering was generated by Raman shifting the fourth harmonic of a Nd:YAG laser (Quanta Ray, DCR-1A). The Raman shifter is composed of a 1-m stainless steel tube (diameter 25 mm), two 25-mm-thick quartz windows, and hydrogen gas at 7.5 atm. The fundamental, second, and fourth harmonics from the Nd:YAG laser were focused into the Raman shifter, and the second anti-Stokes line (218 nm) was selected by a beam separator made of rectangular and Pellin–Broca prisms. The laser power for the 218-nm line was 100–120 μJ/pulse at the sample point. The pump beam for photodissociating the COHb was obtained mostly from a nitrogen laser-pumped dye laser (Molectron UV24-DLII system), which was operated at 419 nm with a dye of $(MS)_2B$ [*p*-bis(*o*-methylstyryl)benzene], and its power was 180 μJ/pulse at the sample point.

The delay time (Δt_d) from the pump pulse to the Raman probe pulse was controlled by a pulse generator (PG) system. BPG in Figure 1 represents a homemade 10-Hz PG consisting of a 1-MHz quartz oscillator (SPG 8640BN) that generates two pulses; one triggers PG1 in Figure 1 (Wavetek, Model 801) and the other triggers PG2 (Hewlett Packard, HP8013B) to fire each laser at the desired time. The actual delay time was determined by putting the partially reflected light of the 419- and 218-nm pulses into the photodiodes PD1 and PD2 (Hamamatsu S1722-02) and by monitoring their output with an oscilloscope. The uncertainty of Δt_d was 1–2 μs. For delay times shorter than 30 ns, the 436-nm pulse generated from the first anti-Stokes H_2 Raman shift of the second harmonic of the Nd:YAG laser was used as the pump beam, and the 218-nm pulse was delayed optically.

The sample was circulated by a peristaltic pump (Mitsumi Scientific Corp. SJ-1211H) at a rate of 3 mL/min, and CO gas was bubbled into the sample reservoir. The sample-illuminating chamber is illustrated in Figure 2. The wire-guided flow system[31] was adopted for all measure-

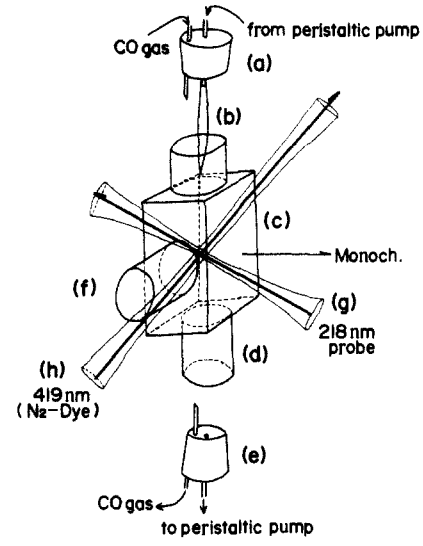

Figure 2. Sample-illuminating chamber: (a) is the cap having the wire-guided flow element and is connected with (b). (c) is a quartz chamber. (e) is the other cap connected to (d). (f) is a manipulation window for setting the wire guide at the correct position and is closed during the measurements. (g) and (h) are the probe and pump beams, respectively.

ments except for calibration of the spectrometer, for which an ordinary quartz cuvette was used. The inside of the chamber was weakly flushed with CO gas for the measurements on COHb. The pump beam was introduced from the back side of the sample plane and illuminated the sample in a rectangular shape (6 × 2 mm^2) by using cylindrical lenses. The probe beam was led from the front side and defocused by two cylindrical lenses; the focal lengths of the horizontal and vertical lenses were 100 and 150 mm, respectively, and the distances between the scattering point and those lenses were 110 and 170 mm, respectively. These illumination optics made the illuminated part of the sample a rectangular shape (4 × 1 mm^2), which produced an image at the entrance slit of the spectrometer similar to the slit size. The 120° back-scattering geometry was adopted. All optical elements were made from Suprasil synthetic quartz.

The scattered light was dispersed with a 1.26-m single monochromator (Spex 1269) equipped with a 2400 groove/mm holographic grating and detected by a UV-sensitive photomultiplier (Hamamatsu R-166UH). The grating was used in the second order. The output from the photomultiplier was averaged by a boxcar integrator (NF BX-531) and transferred to a microcomputer (NEC PC-9801VM). The wavenumbers of the Raman bands were calibrated with acetone, acetonitrile, and cyclohexane as standards.

Hb A was isolated from human adult blood by the usual method,[32] and the minor components were removed by ion-exchange chromatography. The purified Hb A was stored as the CO-bound form at 7 °C and was diluted to a concentration of 400 μM (heme) with 50 mM Tris-HCl buffer, pH 7.4. MetHb A was prepared by addition of potassium ferricyanide, and the excess oxidant was removed by gel filtration. The fluoride adduct (metHbF) was obtained by adding NaF to the metHb solution until a final concentration of NaF of 0.1 M was reached. The sample was replaced with a fresh one every 40 min. Since it took about 20 min for one scan, the fresh sample was incorporated after every two scans.

UV laser irradiation of proteins often causes their degradation.[32] Although in this experiment some efforts were made to lower the photon density of the exciting light at the sample-illuminating spot without losing the total number of photons, it is still important to confirm the integrity of the sample after the Raman measurements. The UV and visible absorption spectra were measured for the sample after 90 min of circulation and 40 min of exposure of the UV laser irradiation (which is the most severe condition in this experiment) and were confirmed to be identical with those of the stock solution (not shown). It is noted that if any damage of the globins had occurred, it should have led to formation of metHb and thus to poorer separation of the α and β bands, but such

(23) (a) Nagai, K.; Kitagawa, T.; Morimoto, H. *J. Mol. Biol.* **1980**, *136*, 271–289. (b) Nagai, K.; Kitagawa, T. *Proc. Natl. Acad. Sci. U.S.A.* **1980**, *77*, 2033–2037. (c) Ondrias, M. R.; Rousseau, D. L.; Kitagawa, T.; Ikeda-Saito, M.; Inubushi, T.; Yonetani, T. *J. Biol. Chem.* **1980**, *257*, 8766–8770.
(24) Baldwin, J.; Chothia, C. *J. Mol. Biol.* **1979**, *129*, 175–220.
(25) Fung, L. W.-M.; Ho, C. *Biochemistry* **1975**, *14*, 2526–2535.
(26) (a) Rava, R. P.; Spiro, T. G. *J. Am. Chem. Soc.* **1984**, *106*, 4062–4064. (b) Rava, R. P.; Spiro, T. G. *Biochemistry* **1985**, *24*, 1861–1865. (c) Rava, R. P.; Spiro, T. G. *J. Phys. Chem.* **1985**, *89*, 1856–1861.
(27) (a) Johnson, C. R.; Ludwig, M.; O'Donnell, S.; Asher, S. A. *J. Am. Chem. Soc.* **1984**, *106*, 5008–5010. (b) Asher, S. A.; Ludwig, M.; Johnson, C. R. *J. Am. Chem. Soc.* **1986**, *108*, 3186–3197.
(28) Bajdor, K.; Peticolas, W. L.; Wharton, C. W.; Hester, R. E. *J. Raman Spectrosc.* **1987**, *18*, 211–214.
(29) Mayne, L.; Hudson, B. *J. Phys. Chem.* **1987**, *91*, 4438–4440.
(30) Su, C.; Park, Y. D.; Liu, G.-Y.; Spiro, T. G. *J. Am. Chem. Soc.* **1989**, *111*, 3457–3459.
(31) Reider, G. A.; Traar, K. P.; Schmidt, A. J. *Appl. Opt.* **1984**, *23*, 2856–2857.
(32) Kilmartin, J. V.; Rossi-Bernardi, L. *Biochem. J.* **1971**, *124*, 31–45.
(33) Johnson, C. R.; Ludwig, M.; Asher, S. A. *J. Am. Chem. Soc.* **1986**, *108*, 905–912.

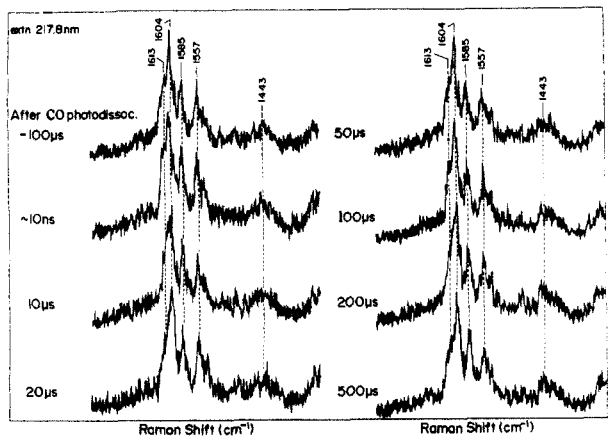

Figure 3. 217.8-nm excited pump–probe RR spectra of COHb in the 1700–1350-cm^{-1} region. The spectra are an average of 8 scans. The delay time between the pump and probe pulses are specified at the left side of each spectrum. The 419-nm pulse was used for the pump beam except for the spectrum of the 10-ns delay for which the 436-nm pulse was used as a pump beam: spectral slit width, 8 cm^{-1}; scan speed, 0.075 nm/min.

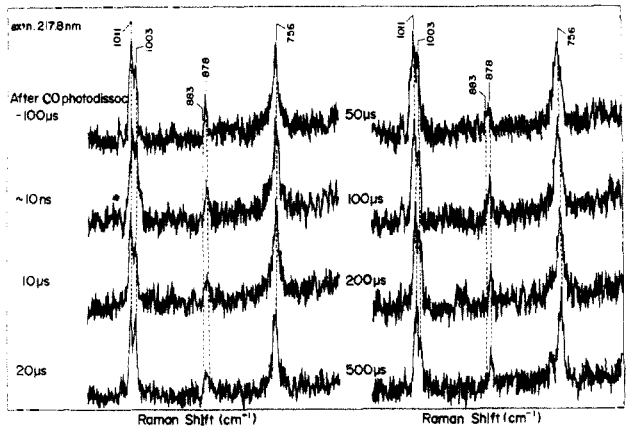

Figure 4. Same experiments as in Figure 4 but in the 1050–650-cm^{-1} region.

a feature was not recognized at all after Raman experiments. Consequently, we believe that sample damage does not take place in the present experiments.

Results

Time-resolved UV RR spectra of COHb in the 1700–1350-cm^{-1} region are shown in Figure 3, where delay times are specified at the left side of each spectrum. Although the pumping system was different for $\Delta t_d = -100$ μs and 10 ns, the two RR spectra were practically the same and they were identical with the spectrum observed in the absence of the pump beam (not shown). The shoulder at 1613 cm^{-1} arises mainly from the Tyr residues (ν_{8a})[34] but contains an appreciable contribution from the Trp residue (ν_{8a} of benzene ring), and its intensity diminished around Δt_d = 10–20 μs. The two intense bands at 1604 (ν_{8a}) and 1585 cm^{-1} (ν_{8b}) are assigned primarily to Phe residues, but Tyr residues might slightly contribute to the 1604-cm^{-1} band (ν_{8b}). The band at 1557 cm^{-1} arises solely from Trp residues, and its intensity seemed to be slightly decreased around Δt_d = 10–20 μs. The broad band around 1440 cm^{-1} also diminished in intensity around Δt_d = 10–20 μs. This band is possibly ascribed to the overtone of amide V[35a] or W6 mode of a Trp residue, which is reported to be sensitive to hydrogen bonding.[35b]

Time-resolved UV RR spectra of COHb in the 1100–600-cm^{-1} region are displayed in Figure 4. It is noted again that the overall

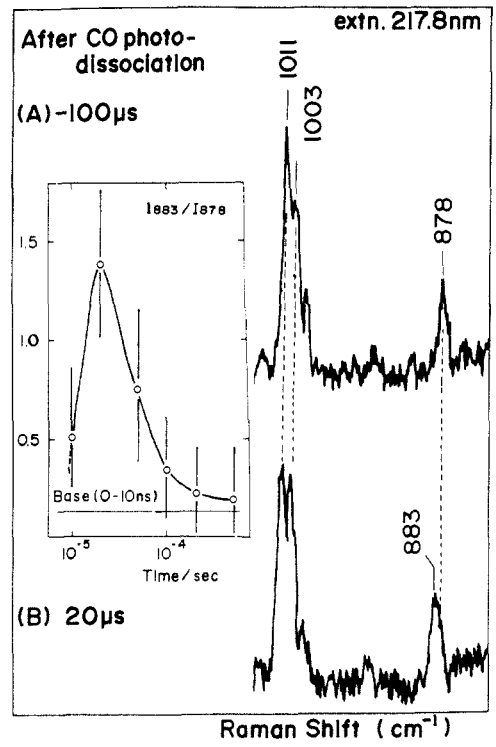

Figure 5. Completely independent results from the pump–probe experiments for two typical values of Δt_d, $\Delta t_d = -100$ μs (upper) and Δt_d = 20 μs (lower), with longer accumulation time (average of 16 scans): pump, 439 nm; probe, 217.8 nm; 100–120 μJ/pulse. The inset figure shows the delay time dependence of the relative peak intensity of the two bands at 883 and 878 cm^{-1} in the spectra displayed in Figure 4. "Base" line means the value obtained from the spectrum for the 10-ns delay. Error bars were estimated from the highest and lowest values in the 8-component spectra.

spectra for $\Delta t_d = -100$ μs and 10 ns resemble each other closely and also resemble the spectrum observed without the pump beam (not shown). The spectrum for Δt_d = 5 μs (not shown) was also close to that for Δt_d = 10 μs. This clearly indicates that the protein structural change does not occur within 10 ns after photolysis, contrary to the earlier report by Dasgupta et al.[8b] The band at 1003 cm^{-1} is assigned to Phe residues, but all other bands are attributed to Trp residues. The relative intensity of the two bands at 1011 and 1003 cm^{-1} remained unaltered until Δt_d = 10 μs, decreased around Δt_d = 10–50 μs, and returned to the original value at $\Delta t_d > 100$ μs. The 878-cm^{-1} band started to decrease in intensity from Δt_d = 10 μs, and a new band appeared at 883 cm^{-1}, but the original pattern was restored at Δt_d = 100 μs. This change would appear as a frequency shift and intensity reduction of the 878-cm^{-1} band if it were measured with a lower spectral resolution, in agreement with the previous observation by Dasgupta et al.,[8b] although the results were retracted due to nonreproducibility.[30]

These observations are essential to elucidate the structural mechanism of hemoglobin cooperativity, but the signal-to-noise ratio in those spectra are not always sufficient to draw an important conclusion. Therefore, we carried out completely independent experiments with different preparation of sample only for two typical values of Δt_d with longer accumulation time. The results are shown in Figure 5, where the spectra for $\Delta t_d = -100$ μs (A) and Δt_d = 20 μs (B) are displayed. The signal-to-noise ratios are much raised partially due to improvements in optical arrangements and partially due to longer accumulation times (16 scans were averaged). Since the intensity reduction of the 1011-cm^{-1} band and the frequency shift of the 878-cm^{-1} band noticed in Figure 4 are well reproduced in Figure 5, other spectra in Figure 4 are also considered to be reliable at the same level and, therefore, are used for further analysis; in the inset of Figure 5, the relative intensities of the two bands of 878 and 883 cm^{-1} are plotted against the delay time. The horizontal line indicates

(34) Fodor, S. P.; Rava, R. P.; Copeland, R. A.; Spiro, T. G. *J. Raman Spectrosc.* **1986**, *17*, 471–475.
(35) (a) Asher, S. A. Private communication. (b) Miura, T.; Takeuchi, H.; Harada, I. *J. Raman Spectrosc.*, in press.

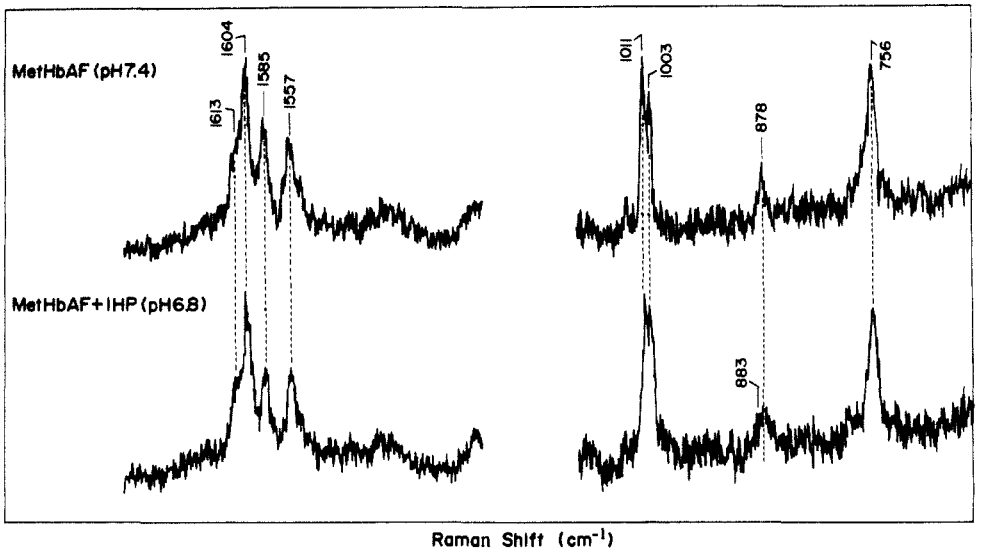

Figure 6. UV RR spectrum of metHbF excited by the single 217.8-nm line. Upper and lower spectra were observed for solutions at pH 7.4 without IHP and pH 6.8 in the presence of 2 mM IHP, respectively.

the value at $\Delta t_d = -100$ μs and 10 ns. Error bars were estimated from the highest and lowest values in the 8-component spectra of each averaged spectrum shown in Figure 4. The relative intensity for $\Delta t_d = 5$ μs was between the values for $\Delta t_d = 10$ ns and $\Delta t_d = 10$ μs, reached a maximum at $\Delta t_d = 20$ μs, and decreased to its initial value. This restoration is due to the regeneration of the CO-bound form in the sample-illuminating chamber. If the sample-illuminating chamber were filled with nitrogen or argon gas, the complete relaxation process from COHb to deoxyHb would have been obtained, and slight modification of the sample chamber for this purpose is under development.

The Raman spectral change observed for $\Delta t_d = 0$ to 20 μs is presumably caused by the quaternary structure change, but in order to confirm it, metHbF was investigated. X-ray crystallographic analysis of metHbF[36] revealed that it adopts the T state in the presence of inositol hexaphosphate (IHP) at pH 6.4 and the R state in its absence at pH 7.4. The 218-nm excited RR spectra of metHbF under the corresponding two solution conditions are shown in Figure 6. Although the intensity of the 1613-cm^{-1} band does not seem to change sensitively in the two spectra, in the presence of IHP the relative intensity of the Trp band at 1011 cm^{-1} to the Phe band at 1003 cm^{-1} became smaller, and also the 878-cm^{-1} band of the Trp residue appeared broader due to the presence of the new band at 883 cm^{-1}. Although the previous report about metHbF by Copeland et al.[8a] which was also retracted recently,[30] did not point out this frequency shift clearly, their apparent spectral changes shown in Figure 1 of their paper[8a] would be consistent with the present observations if one considers that the present spectra are of higher resolution. Consequently, we can conclude that the UV RR spectral change from $\Delta t_d = 0$ to 20 μs is caused by the R to T transition of the quaternary structure.

Discussion

The 218-nm excited RR spectra of Hb provided some Raman bands of aromatic residues Phe, Tyr, and Trp. (There are 6 Tyr, 15 Phe, and 3 Trp residues per $\alpha\beta$ dimer of Hb A.) Johnson et al.[33] have warned that UV excitation of aromatic residues by a pulsed laser might produce photoionization products such as tyrosyl and tryptophanyl radicals, whose strongest bands would occur at 1502 and 1646 cm^{-1}, respectively. Since such bands were not found in the present spectra, photoionization products need not be considered in interpretation of the present results. It has also been reported that intensity saturation takes place at higher laser powers for the probe beam.[33] Since the present power range is rather low already, we could not obtain a spectrum of good quality when the laser power was further lowered. Although the power dependence could thus not be examined in the present study, all the measurements were carried out similarly with the practical lowest limit of laser power and, therefore, the observed intensity change of the Raman bands upon change of the delay time would not be caused by saturation effects.

The change of the UV RR bands took place around 10–20 μs after the photolysis but not at all before 10 μs. This feature is in agreement with Spiro and co-workers' new conclusion.[30] However, the present results do not support their conclusion about the presence of an intermediate around $\Delta t_d = 10$ μs; the relative intensity of the Trp bands around 880 cm^{-1} for $\Delta t_d = 5$ μs falls in with the reasonable position extrapolated from the curve shown in Figure 5, and an overall spectral pattern for $\Delta t_d = 5$ μs was not unusual in comparison with the spectra for $\Delta t_d = 10$ ns and 10 μs. Although the Trp and Tyr bands may reflect different features of a structural change, it is desirable to follow the complete change from the ligated R to deoxy T structure in order to point out the presence of an intermediate. Therefore, we did not pursue this problem further in this study. Anyway, it is now established that changes of the globin structure do not occur on a nanosecond time scale.

The most prominent RR spectral changes upon the quaternary structure change were observed for the 878-cm^{-1} band of Trp at $\Delta t_d = 10$–20 μs. According to the normal-coordinate analysis, the 878-cm^{-1} band of Trp is associated with motions of the NH group as well as of the benzene ring, and therefore this band can be sensitive to hydrogen bonding.[37] Indeed, the Raman intensity of this band of other proteins upon visible excitation was noted to be sensitive to the Trp environment; the band becomes weaker as Trp is exposed.[38] In the present study, the 878-cm^{-1} band became weaker and a new band grew in on its higher frequency side in the deoxy form and in metHbF with the T structure. This implies that the part of the Trp residues responsible for the 878-cm^{-1} band underwent a structural change and gave rise to the corresponding band at higher frequency, presumably due to the formation of a hydrogen bond at the NH group of the indole ring. Among the three Trp residues at α14 (A12), β15 (A12), and β37 (C3), the former two are hydrogen bonded within a subunit irrespective of the two quaternary structures[24] and probably would not exhibit a change of their RR spectra upon photodissociation. In contrast, the β37-Trp is located at the α_1–β_2 interface where this residue is in contact with $\alpha_1$140-Tyr, $\alpha_1$94-Asp, and $\alpha_1$95-Pro in the deoxy state but is freed from the $\alpha_1$140-Tyr contact in the oxy state. In fact, the UV absorption differences between the T and R states of deoxyHb[39a] and metHb[39b] were

(36) Fermi, G.; Perutz, M. F. *J. Mol. Biol.* **1977**, *114*, 421–431.

(37) Miura, T.; Takeuchi, H.; Harada, I. *Biochemistry* **1988**, *27*, 88–94.

(38) Kitagawa, T.; Azuma, T.; Hamaguchi, K. *Biopolymers* **1979**, *18*, 451–465.

ascribed satisfactorily to environmental changes of β37-Trp and α42-Tyr. Since simple changes in dielectric field might induce intensity changes of Raman bands but not a noticeable frequency shift, we infer that changes of β37-Trp should involve a change of the hydrogen bonding at the NH group so that it could exhibit an appreciable frequency shift. Since β37-Trp (C2) is in contact with the α subunit at the FG corner, it is highly likely that the movement of proximal His (F8) upon ligation or deligation of the sixth ligand (O_2 or CO) is conveyed to the subunit surface through the F helix.

The 1604-cm^{-1} band in Figure 3 is associated with the split ν_8 band of benzene ring of Tyr and Phe. In the 218-nm excited RR spectra of amino acid solutions containing a known amount of perchlorate ions (used as an internal intensity standard), which were obtained in the same instrumental conditions as the present experiments (not shown), the intensity ratio of the 1613-cm^{-1} band to the 1557-cm^{-1} band of Trp was 0.3, and the intensity of the ν_{8a} band of Tyr was greater than that of the 1557-cm^{-1} band by a factor of 5. Therefore, the intensity contribution of Trp residues to the shoulder at 1613 cm^{-1} would not be large. This shoulder would rather arise from the high-frequency counterpart of the split ν_8 band of Tyr (ν_{8a}). However, it should be noted that the intensities of the ν_8 bands of Phe and Tyr were alike in the 218-nm excited RR spectra of amino acid solutions with an intensity standard, and the number of Phe residues is more than twice as large as Tyr residues for Hb A. Accordingly, the major part of intensity of the 1604-cm^{-1} band in Figure 3 would arise from Phe residues.

The 1011-cm^{-1} band of Trp arises from the breathing-like vibration of the benzene ring.[37] The intensity reduction of this band and other Trp bands may imply a decrease in the absorbance at 218 nm and thus a stacking of the Trp with other aromatic residues. Such stacking would also interpret the intensity reduction of the 1613-cm^{-1} shoulder if the band were due to the Trp contribution. Alternatively, if the shoulder were due to the Tyr contribution, it would be attributed to α42-Tyr as explained by Su et al.[30] Further investigation with a mutant Hb is desirable.

For either assignment, it became evident that environmental changes of the aromatic residues at the α_1-β_2 interface occurred at 10-20 μs after the photolysis. This is consistent with the results from kinetic absorption studies,[12,14] which pointed out that the quaternary structure changes around 20 μs after the photolysis of COHb. However, there are evidences for faster changes of the structure. A deoxyHb-like visible absorption spectrum is generated with a time constant of 0.35 ps.[15a] Hofrichter et al.[14] pointed out from a transient absorption study the presence of two other relaxations with time constants of 100 and 800 ns. The RR ν_{Fe-His} frequency relaxes in the time range from 10 ns to 1 μs,[20b,c] but the porphyrin skeletal stretching frequencies associated with the core size of porphyrin (ν_{10}, ν_{11}, and ν_{19}) relax in the time range between 20 and 300 ns.[19b,c] In the present measurements, data are lacking in the time range between Δt_d = 10 ns and 5 μs, where some other delay technique would be required, but it should be emphasized the amount of the changes occurring during this period is one-third of that occurring between 10 and 20 μs. Due to rebinding of CO to the photodissociated species, the complete curve describing the behavior after photolysis could not be derived from the present experiments. In addition, there are a few other small spectral changes that may reflect structural changes different from those discussed here, but their poor signal-to-noise ratio did not allow us to discuss them at the present stage. A more detailed study with the improved sample chamber is in progress.

In conclusion, the present observations strongly suggest that the ligand dissociation from the heme iron is communicated to the F helix through the Fe-His bond, and the movement of the F helix causes a change in the α_1-β_2 contact. It is unlikely that the dissociated CO triggers the quaternary structure change through the interaction with the distal His (E7).

Acknowledgment. We express our gratitude to Prof. Hideki Morimoto of Osaka University for stimulating discussion and to Dr. John Hougen of National Bureau of Standards for reading the manuscript.

Registry No. Inositol hexaphosphate, 83-86-3.

(39) (a) Perutz, M. F.; Ladner, J. E.; Simon, S. R.; Ho, C. *Biochemistry* **1974**, *13*, 2163-2173. (b) Perutz, M. F.; Fersht, A. R.; Simon, S. R.; Roberts, C. K. *Biochemistry* **1974**, *13*, 2174-2185.

Unequivocal Proof of Slowed Chromium Tricarbonyl Rotation in a Sterically Crowded Arene Complex: An X-ray Crystallographic and Variable-Temperature High-Field NMR Study of $(C_6Et_5COCH_3)Cr(CO)_3$

Patricia A. Downton, Bavani Mailvaganam, Christopher S. Frampton, Brian G. Sayer, and Michael J. McGlinchey*

Contribution from the Department of Chemistry, McMaster University, 1280 Main Street West, Hamilton, Ontario, Canada L8S 4M1. *Received March 20, 1989*

Abstract: The low-temperature ^{13}C NMR spectrum of $(C_6Et_5COCH_3)Cr(CO)_3$ is explicable only in terms of a single stereoisomer, i.e., the 1-proximal-acetyl-2,4,6-distal-3,5-proximal conformer. The $Cr(CO)_3$ resonance is split 2:1 both in solution at −100 °C and in the CPMAS solid-state spectrum at 30 °C; these data demonstrate that $Cr(CO)_3$ rotation has stopped on the NMR time scale. Crystals of $(C_6Et_5COCH_3)Cr(CO)_3$ are triclinic, of space group $P\bar{1}$ with a = 8.876 (2) Å, b = 9.458 (3) Å, c = 13.383 (4) Å, α = 95.26 (2)°, β = 98.89 (2)°, γ = 111.54 (2)°, V = 1018.9 (5) Å^3, D_c = 1.29 g cm^{-3}, D_m = 1.28 g cm^{-3} for Z = 2, and R_1 = 0.0659 (R_2 = 0.0753) for 2673 unique reflections (R_1 = 0.0501, R_2 = 0.0547 for 2198 reflections with $I > 2.5\sigma(I)$). The alternating proximal-distal arrangement of substituents is in accord with the NMR data. These results are discussed in the context of previous reports on $(C_6Et_6)Cr(CO)_2L$ complexes.

The dynamic behavior of tricarbonyl(η^6-hexaethylbenzene)-chromium, **1**, in solution has been the subject of some debate over a period of several years. In 1979 we reported the solid-state ^{13}C NMR spectrum of **1** and noted that the methyl, methylene, and ring carbon resonances were not single peaks but instead appeared as pairs of equally intense lines.[1] This observation was interpreted

0002-7863/90/1512-27$02.50/0